

APPLICATION OF COMPUTATIONAL FLUID DYNAMICS TO SIMULATE CAVITATING FLOW AROUND HYDROFOIL

Mohammad Shakil Ahmmed¹ and M. M. Karim²

¹HTB (Bang.) Ltd, Dhaka, Bangladesh,

² Dept. of Naval Architecture and Marine Engineering, BUET, Dhaka, Bangladesh

ABSTRACT

In this research, flow around hydrofoil in non-cavitating and cavitating condition is simulated using computational fluid dynamics (CFD). The aim is to capture the flow features and hydrodynamic characteristics of flow around hydrofoil in both steady and unsteady condition. Two dimensional finite volume method (FVM) is applied for solving this problem. To describe the generation and evaporation of vapor phase, a bubble dynamics cavitation model is chosen. To capture turbulent boundary layer along the hydrofoil surface, RNG $k-\varepsilon$ turbulence model with enhanced wall treatment is used. The method is applied on NACA 0012 hydrofoil section and predicted results are validated by comparing with the numerical/experimental result published by other researchers. It may be concluded that the method predicts steady/unsteady cavitating flow around hydrofoil very well.

Keywords: Computational Fluid Mechanics, Finite Volume Method, Cavitation, Hydrofoil, Turbulence .

1. INTRODUCTION

The major benefit of CFD analysis is its ability to compute the values of every flow parameter at each grid point in the domain studied, giving a very descriptive picture of the entire flow field. The cavitation is a very important phenomenon for the performances of underwater propellers and hydrofoils. When the flow past the surface of marine propeller, the cavity bubbles generate at the low pressure zone where the local pressure is lower than the vapor pressure. The cavity bubbles make the propeller thrust breakdown, vibrations, noises and erosion as they move to the high pressure zone. For that reason, the issue of cavitation for the ship hydrodynamic is a very important research topic.

Cavitation modeling through the computational method has been done for many years. Potential flow theory was primarily used for simulating cavity flow and it is still used in many engineering applications. The numerical computations of cavity flow have become possible due to the fast growing of computational capabilities. And thus the studies of cavitation modeling through the computation of the Navier-Stokes (N-S) equations have been emerged in the last decade. Kubota et al. [1] had established a multi-phase flow cavitation model which based on the mixture density and void fraction. The two phase cavitation model was applied to compute partial cavitation and super cavitation flows. Senocak and Shyy [2] presented the numerical simulations of cavitating flows based on the finite volume method for solving Navier-Stokes equations. Singhal et al. [3] developed a mixture cavitation model and used by the commercial software FLUENT. The cavitation model has considered the effects of the

turbulent fluctuation, bubble dynamics and non condensable gases. On the other hand, Chahine and Hsiao [4] proposed the combination of boundary element method and viscous flow calculation.

To investigate the cavitation phenomena and validate the numerical procedures, a number of investigations were performed in the past by Kubota et al. [1], Alajbegovic et al. [5], Stutz et al. [6], Schnerr et al. [7], and Frobenius et al. [8]. For numerical simulation of cavitating flow, various methods were developed and most of the studies treated the two phase flow as a single vapor-liquid phase mixture flow. The evaporation and condensation can be modeled with different source terms that are usually derived from the Rayleigh-Plesset bubble dynamics equation. This approach was first made by Kubota et al. [1] who used the linear part in the Rayleigh-Plesset equation to describe the evaluation of bubble radius as a function of the surrounding pressure. Other cavitation models which included more complex relation between pressure and bubble radius were derived from the Rayleigh-Plesset equation by Schnerr et al. [7] and Frobenius et al. [8], but they all include some quantities (like bubble number density and initial bubble diameter) which are very hard to determine. For example the recommended value for bubble number density that has to be included in the mentioned model is according to Kubota et al., according to Schnerr and Sauer or to Frobenius et al and even according to Alajbegovic et al [6]. Recently, Singhal et al. [3] and Kunz et al. [9] proposed to consider a transport equation model for the void ratio, with vaporization/condensation source terms to control the mass transfer between the two phases. This method has the advantage that it can take into account the time

influence on the mass transfer phenomena through empirical laws for the source term. It also avoids using quantities like bubble number density and initial bubble diameter. The other way to model cavitation process is by so called barotropic state law that links the density of vapor-liquid mixture to the local static pressure. The model was proposed by Delannoy and Kueny [10] and later widely used by Song et al. [11], Hofmann et al. [12], Lohrberg et al. [13] and Coutier-Delgosha et al. [14]. The results obtained with the barotropic cavitation model show very good correlation to the experiments but the past simulations lacked in robustness of the numerical algorithms, which resulted in numerical instability and sometimes, poor convergence. A cavitation model, based on bubble dynamics equation proposed by Singhal et al. [3] is used for computation of cavitating flows. In the present studies, the non-cavitating operation is first characterized in details as a reference for cavitating conditions. Four cavitating conditions are separately analyzed: $\sigma=1.0$ & 2.0 where an unsteady partial cavitating behavior is obtained and $\sigma=0.4$ & 0.2 where a super-cavitating flow is observed.

2. NUMERICAL SIMULATION

The numerical model uses an implicit finite volume method associated with multiphase and cavitation model. For numerical simulation of cavitating flow, a bubble dynamics cavitation model is used to describe the cavity formation. The RNG k- ϵ turbulence model with enhanced wall treatment is used to capture the turbulent boundary layer. The Reynolds number ($Re=10^6$) based on chord length is used. A second order central scheme is used for discretization of space except convection terms. The convective term in the momentum equation is discretized by the QUICK scheme for non cavitating flow and second order implicit scheme is used for cavitating problem. Pressure based solver SIMPLE is used as the velocity pressure-coupling algorithm.

3. MULTIPHASE MODEL

A single fluid (mixture model, Dular et al., 2005 [15]) approach is used. It consists of using standard (Navier–Stokes) viscous flow equation and conventional turbulence model (RNG k- ϵ model). The mass and momentum conservation equations (Eqns. 3 and 4) together with the transport equation (Eq. 5) and the equation of the turbulence model form the set of equations from which fluid density (which is the function of the vapor mass fraction f_v) is computed

The $\rho_m - f_v$ (mixture density-vapor mass fraction) relation is:

$$\frac{1}{\rho_m} = \frac{f_v}{\rho_v} + \frac{1-f_v}{\rho_l} \quad (1)$$

The volume fraction of the vapor phase (α_v) is related to the mass fraction of the vapor phase with:

$$\alpha_v = f_v \frac{\rho_m}{\rho_v} \quad (2)$$

The mass conservation equation for the mixture is:

$$\frac{\partial}{\partial t}(\rho_m) + \nabla \cdot (\rho_m \vec{v}_m) = 0 \quad (3)$$

The momentum conservation equation for the mixture is

$$\frac{\partial}{\partial t}(\rho_m \vec{v}_m) + \nabla \cdot (\rho_m \vec{v}_m \vec{v}_m) = -\nabla p + \nabla \cdot [\mu_m (\nabla \vec{v}_m + \nabla \vec{v}_m^T)] + \rho_m \vec{g} + \vec{F} \quad (4)$$

And the transport equation for the vapor is:

$$\frac{\partial}{\partial t}(\rho_m f_v) + \nabla \cdot (\rho_m \vec{v}_m f_v) = R_e - R_c \quad (5)$$

4. CAVITATION MODEL

The working fluid is assumed to be a mixture of liquid, liquid vapor and noncondensable gas. The vapor mass fraction is the dependent variable in the transport equation. The source terms R_e and R_c which are included in the transport equation define vapor generation (liquid evaporation) and vapor condensation, respectively. Source terms are the function of the local flow condition (Static pressure, velocity) and fluid properties (liquid and vapor phase densities, saturation pressure and liquid vapor surface tension). The source terms are derived from the Rayleigh-Plesset equation where higher order terms and viscosity term have been left out. The source terms can be expressed as-

$$R_e = C_e \frac{\sqrt{k}}{\gamma} \rho_l \rho_v \sqrt{\frac{2}{3} \frac{p_v - p}{\rho_l} (1 - f_v - f_g)} \quad \text{when } p < p_v \quad (6)$$

$$R_c = C_e \frac{\sqrt{k}}{\gamma} \rho_l \rho_l \sqrt{\frac{2}{3} \frac{p_v - p}{\rho_l} f_v} \quad \text{when } p > p_v \quad (7)$$

5. COMPUTATIONAL DOMAIN

Figure 1 which shows a schematic view of the NACA0012 hydrofoil geometry. The two-dimensional configuration is mounted at 10 degree angle-of-attack. The equation for the upper surface of the symmetric foil geometry hydrofoil is provided as:

$$\frac{y}{c} = a_0 \sqrt{\frac{x}{c}} + a_1 \left(\frac{x}{c}\right) + a_2 \left(\frac{x}{c}\right)^2 + a_3 \left(\frac{x}{c}\right)^3 + a_4 \left(\frac{x}{c}\right)^4$$

$$\bar{y} = a_0 \sqrt{\bar{x}} + a_1 (\bar{x}) + a_2 (\bar{x})^2 + a_3 (\bar{x})^3 + a_4 (\bar{x})^4$$

With $a_0= 0.11858$, $a_1= -0.02972$, $a_2= 0.00593$, $a_3= -0.07272$, $a_4= -0.02207$, $\bar{y} = y/c$ and $\bar{x} = x/c$ is the dimensionless coordinate along the chord line. The flow from left to right with the hydrofoil of chord length $c=1$

m submerged in an incompressible fluid is considered. The computational domain is sketched in Fig.1. The hydrofoil is located in the middle of a channel of lengths at left and right sides of the foil are 25c and 30c respectively.

Fig. 1 also shows the 2D computational domain and boundary conditions. The inlet boundary condition is specified as 'velocity inlet' with a constant velocity profile. Upper and lower boundaries are also considered as 'velocity inlet'. The outlet uses a constant pressure boundary condition. The foil itself is a 'no-slip wall', i.e., $u = 0, v = 0$ at the foil surface. In the physical domain the flow is not confined. Nevertheless, a fictitious external rectangular boundary is needed at a large distance from the hydrofoil in order to solve the governing equations numerically. Also the flow at exit is treated as a pressure outlet. The problem setup together with the boundary condition is shown in Fig. 1.

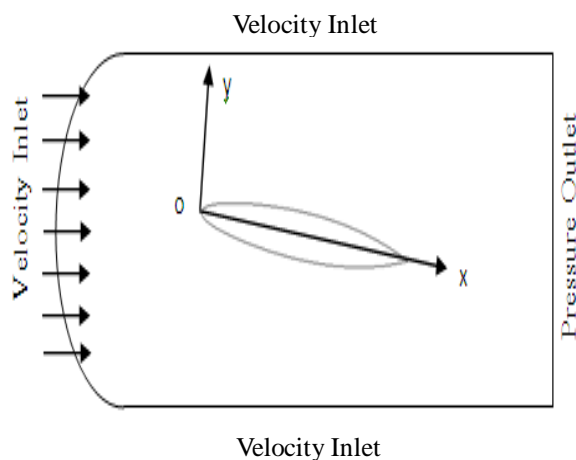


Fig 1. Schematic diagram of the flow field around NACA0012 Hydrofoil with boundary conditions

A 2-block C-type orthogonal grid, fined in the expected cavity area and solid boundary, is used as shown in Fig. 2. This type of grid is particularly beneficial for pressure-driven and stagnation oriented flow due to its good leading edge resolution features. This particular mesh has approximately 17080 nodes, 33880 faces and 16800 quadrilateral cells with considerable mesh concentrated both around the hydrofoil and in the wake.

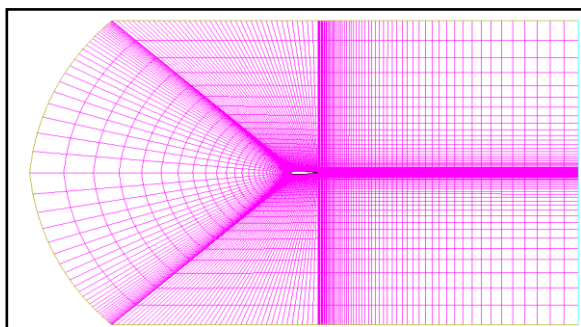


Fig. 2. Computational domain

6. RESULT AND DISCUSSION

The present study can be classified into two main

parts: Firstly, the non cavitating flow and secondly cavitating flow over the proposed NACA0012 hydrofoil. The present method is considered relevant to the analysis of complex cavity flows, because it can treat the whole flow fields at once. In the simulation of the flow features, a computer code developed with C++ is used in the research. For numerical simulations the parameters used are: Reynolds number based on chord length $Re=10^6$, uniform flow velocity 7 m/s, water temperature 293.15 K etc. The numerical model uses an implicit finite volume method based on a SIMPLE algorithm of Patankar [16], associated with multiphase and cavitation model. The RNG k- ϵ turbulence model with enhance wall treatment is used to capture turbulence boundary layer.

A second order central scheme is used for discretization of space except the convective terms. The convective term in the momentum equation is discretized by the QUICK scheme for non cavitating flow and second order implicit scheme is used for cavitating problem.

The convergence criterion is determined by observing the evaluation of different flow parameters (velocity magnitude at inlet, static pressure behind the hydrofoil) in the computational domain. For convergence, each value of residual is taken as 10^{-4} . Time step size has a great influence on simulation of cavitating flow. Different time step values are tested, eventually the time step for computation is set to 5×10^{-5} and approximately 30 iterations per time step are needed to obtain a converged solution.

For validating the present method, the computed result is compared with the experimental value of Takasugi et al. [17], where the computation is done at different angles of attack of the hydrofoil at steady condition. Fig. 3 shows the comparison of the present values of lift co-efficient (C_L) at different angles of attack with the experimental values. The result shows a good agreement on the predictions.

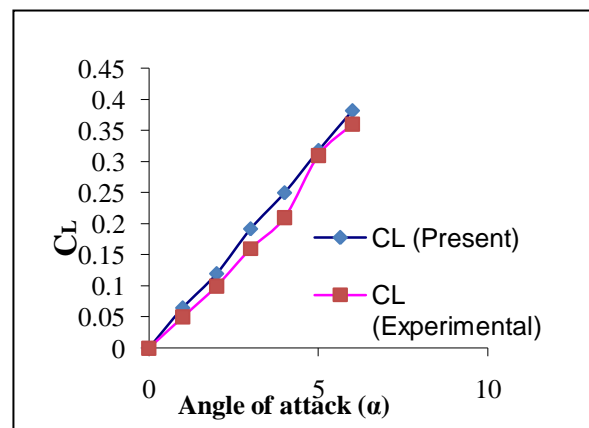


Fig. 3. Comparison of lift co-efficient with the experimental value at various angles of attack

To predict the behavior of the cavitating flow for different values of cavitation number such as $\sigma = 0.2, 0.4, 0.6, 0.8, 1.0, 1.2, 1.4, 1.6, 1.8$ & 2.0 the numerical simulation is carried out. For validation of the present method at cavitating condition, the simulation is done at

different cavitation number at 10 degree angle of attack to compare with the experimental value by Takasugi et al. [17] and numerical value by Ghassemi [18] in steady condition. Fig. 4 shows the value of the present C_L and C_D and comparison with the value of the other researchers. From the figure, it is clear that the value of C_L is quite similar with the experimental and other values, especially at $\sigma = 1.2$ and 1.4 and also the value of C_D similar to the value of other researchers.

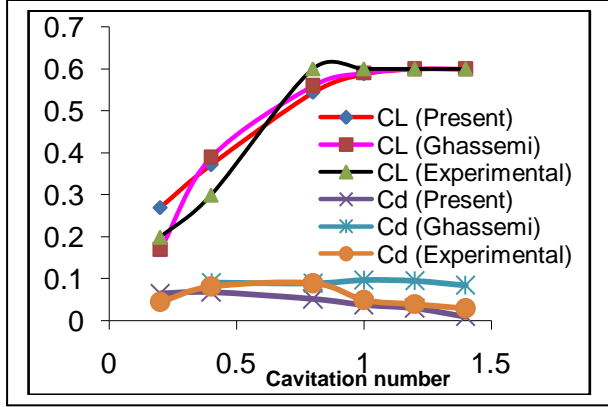


Fig 4. Comparison of lift coefficient (C_L) & drag coefficient (C_D) at various cavitation number (σ) at $\alpha=10$ deg. with the value of other researchers

After performing the steady condition, the drag and lift co-efficient also calculated in unsteady condition. The intention of the simulation is to predict the behavior of the cavity in unsteady condition. Fig. 5 shows the convergence of the lift and drag force at $\sigma=1.0$ at 10 degree angle of attack. From the figure it is clear that the flow is converged.

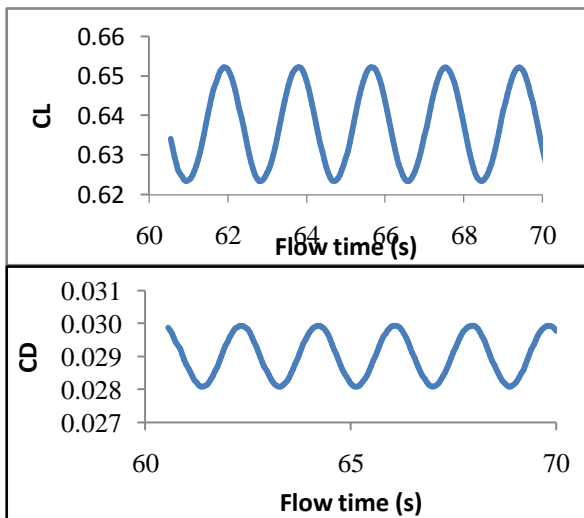


Fig 5. Convergence of the Lift and drag co-efficient

Table 1 shows the values of lift and drag co-efficient in unsteady condition at 10 degree angle of attack. From the values of lift and drag force it is clear that , with increasing the cavitation number (σ), increase the lift force and on the other hand decrease the drag force.

Table 1: Lift and Drag co-efficient at unsteady condition ($\alpha=10$ degree)

Cavitation Number (σ)	\bar{C}_L	\bar{C}_D
0.2	0.398	0.069
0.4	0.419	0.070
0.6	0.555	0.070
0.8	0.587	0.048
1.0	0.636	0.029
1.2	0.697	0.012

The time average values are computed over a range of time. First, the maximum cavity length $\bar{l}_{max} = \frac{l_{max}}{C}$, the maximum cavity thickness $\bar{t}_{max} = \frac{t_{max}}{C}$, the position of maximum cavity thickness $\bar{lt}_{max} = \frac{lt_{max}}{l_{max}}$ and the abscissa of cavity detachment $\bar{ld} = \frac{ld}{C}$ are identified in order to confirm the aspect of the qualitative flow field at cavitation number. Table 2 shows the summary of the cavitation parameter. As decreasing the cavitation number, the maximum cavity length become longer and its thickness thicker.

Table 2: Summary of the cavitation parameter

σ	\bar{l}_{max}	\bar{t}_{max}	\bar{lt}_{max}	\bar{ld}
2	0.109	0.025	0.688	0.002
1.8	0.125	0.045	0.728	0.002
1.6	0.152	0.061	0.690	0.002
1.4	0.213	0.075	0.549	0.002
1.2	0.286	0.102	0.475	0.003
1.0	0.518	0.194	0.451	0.019
0.8	0.945	0.497	0.445	0.002

The pressure co-efficient curve for cavitation number $\sigma=0.2, 0.4, 1$ and 2 are shown in Fig. 6. Pressure remains constant as long as the cavitation number is smaller and as the cavitation number is increased, the pressure fluctuates and this causes the pressure varies on the foil surface. At cavitation number $\sigma=0.2$ and 0.4 the pressure remains constant, and at $\sigma=1$ and 2 the pressure shows fluctuation.

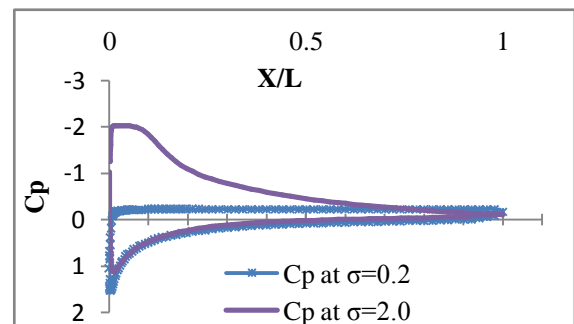


Fig 6(a). Pressure co-efficient (C_p) at $\sigma=0.2$ and 2

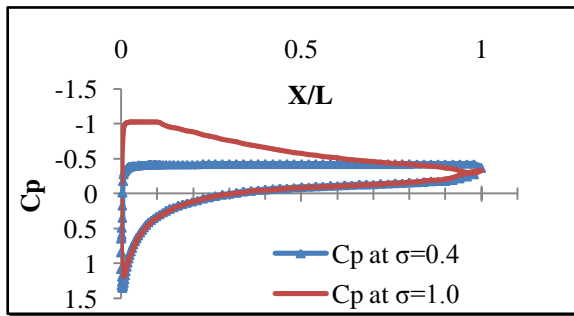


Fig 6(b): Pressure co-efficient (C_p) at $\sigma=0.2, 0.4, 1$ and 2

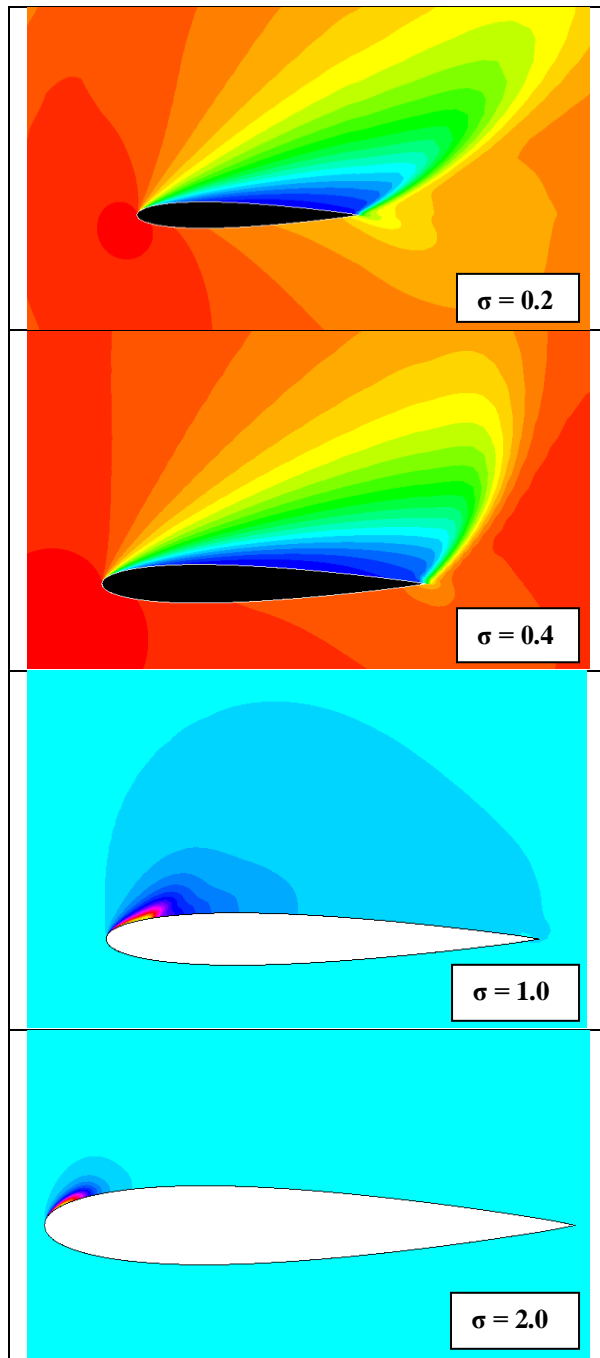


Fig. 7: Density contour at $\sigma=0.2, 0.4, 1$ and 2

The density contours for cavitation number $\sigma=0.2, 0.4, 1$ and 2 are shown in Fig. 7. These contours show the

expansion of cavity and their sizes for different cavitation number. At $\sigma=0.2$ and 0.4 the cavity length remains larger and, extends to a larger region of the foil surface. As a result, super cavitation occurs and pressure remains constant. But as the cavitation number increases, causes the pressure fluctuation and pressure varies on the foil surface. At $\sigma=1$ and 2 partial cavitation occurs.

7. CONCLUSION

Two-dimensional finite volume method has been applied to simulate incompressible flow around NACA0012 hydrofoil. The method seems very prospective for simulation of flow around hydrofoil in both non-cavitating and cavitating conditions. The lift and drag co-efficient are computed in both cavitating and non-cavitating condition. It is observed that the RNG $k-\epsilon$ Turbulence model with enhanced wall treatment computes the lift and drag co-efficient almost accurately. The pressure distributions along the foil surface and the density contour are also predicted to capture the flow features. The computed results show good agreement with experimental and numerical results published by other researchers.

8. REFERENCES

1. Kubota, A., Hiroharu, K., Yamaguchi, H., 1992, "A New Modeling of Cavitating flows, a Numerical Study of Unsteady Cavitation on a Hydrofoil section", *J. Fluid Mech.* 240, 59–96.
2. Senocak, I., and Shyy, W., 2001, "Numerical Simulation of Turbulent Flows with Sheet Cavitation," CAV2001, Proc. 4th International Symposium on Cavitation, CAV2001A7.002, California Institute of Technology, Pasadena, CA, (<http://cav2001.library.caltech.edu>).
3. Singhal, A. K., Athavale, M. M., Li, H. Y., 2002, "Mathematical Basis and Validation of the Full Cavitation Model", *Journal Fluid Engineering*, Vol. 124, No. 3, pp. 617–624.
4. Chahine, G.L. & Hsiao, C.T., 2000, "Modeling 3D unsteady sheet cavities using a coupled UnRANS–BEM code", In Proc. 23rd ONR Symposium on Naval Hydrodynamics.
5. Alajbegovic, A., Groger, H.A., Philipp, H., 1999, "Calculation of Transient Cavitation in Nozzle using the Two-Fluid model", in: 12th Annual Conference on Liquid Atomization and Spray Systems, Indianapolis, IN, USA.
6. Stutz, B., Reboud, J. L., 2000, "Measurements within unsteady cavitation", *J. Exp. Fluids*, 29: 545-552.
7. Schnerr, G.H., Sauer, J., 2001, "Physical and Numerical Modeling of Unsteady Cavitation Dynamics", in: 4th International Conference on Multiphase Flow, ICMF-2001, New Orleans, USA.
8. Frobenius, M., Schilling, R., Bachert, R., Stoffel, B., 2003, "Three-Dimensional, Unsteady cavitation effects on a single Hydrofoil and in a radial Pump – Measurements and Numerical Simulations", Part two: Numerical simulation, in: Proceedings of the Fifth International Symposium on Cavitation, Osaka, Japan.

9. Kunz, R., Boger, D., Chyczewski, T., Stinebring, D., Gibeling, H., 1999, "Multi-phase CFD Analysis of Natural and Ventilated Cavitation about Submerged Bodies", ASME FEDSM99-7364 ASME FEDSM99-7364, SAN Francisco.
10. Delannoy, Y., Kueny, J.L., 1990, "Two Phase Flow Approach in Unsteady Cavitation Modeling", in: Cavitation and Multiphase Flow Forum, ASME FED, vol. 98, pp. 153–158.
11. Song, C. C., He, J., 1998, "Numerical simulation of cavitating flows by single-phase flow approach", in: 3rd International Symposium on Cavitation, Grenoble, France, pp. 295–300.
12. Hofmann, M., Lohrberg, H., Ludwig, G., Stoffel, B. B., Reboud, J.L., Fortes-Patella, R., 1999, "Numerical and Experimental Investigations on the Self – Oscillating behaviour of Cloud Cavitation – Part 1: Visualisation", in: Proceedings of the 3rd ASME/JSME Joint Fluids Engineering Conference, San Francisco, CA.
13. Lohrberg, H., Stoffel, B., Fortes-Patella, R., Reboud, J.L., 2002, "Numerical and Experimental Investigations on the Cavitation flow in Cascade of Hydrofoils", Exp. Fluids 33, 578–586.
14. Coutier-Delgosa, O., Fortes-Patella, R., Reboud, J.L., 2003, "Evaluation of Turbulence Model Influence on the Numerical Simulations on Unsteady Cavitation", J. Fluids Engrg. 125, 38–45.
15. Dular, M., Bacher, R., Stoffel, B., Sirok, B., 2005, "Experimental Evaluation of Numerical Simulation of Cavitating Flow Around Hydrofoil", European Journal of Mechanics B/Fluids 24, 522-538.
16. Patankar, S.V., 1980, "Numerical Heat Transfer and Fluid Flow", Hemisphere, Washington DC.
17. Takasugi, N., Yamaguchi, H., Kato, H. and Maeda, M., 1992, "An experiment of cavitating flow around a finite span hydrofoil", Society of Naval Architects of Japan, 172, pp 257-265 (in Japanese)
18. Ghassemi, H., 2003, "Boundary Element method applied to the cavitating hydrofoil and marine propeller", Scientia Iranica, Vol.10, No.2, and PP: 142-152.

9. NOMENCLATURE

Symbol	Meaning	Unit
C_L	Lift co-efficient	-
C_D	Drag co-efficient	-
C_p	Pressure co-efficient	-
C_{1e}	Turbulent constant	-
C_{2e}	Turbulent constant	-
σ	Cavitation number	-
L	Length	Meter
C	Chord length	Meter
T	Thickness	Meter
α	Angle of attack	Degree
Re	Reynolds number	-
P	Pressure	Pa
ρ	Density	Kg/m^3
f_v	Vapor mass fraction	-
f_g	Gas mass fraction	-

10. APPENDIX

Hydrodynamic parameters are given in Fig A.1.

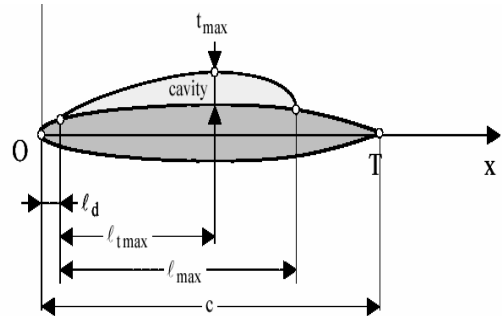


Fig A.1. Two dimensional definitions of l_{max} , l_{tmax} , t_{max} and l_d

11. MAILING ADDRESS

Mohammad Shakil Ahmmed

HTB (Bang.) Ltd, 210/2, Dr. Kudrat-E-Khuda Road
Suite: 4E, Dhaka, Bangladesh,

E-mail: ahmmedshakil@gmail.com

M. M. Karim

Dept. of Naval Architecture and Marine Engineering,
BUET, Dhaka-1000,

E-mail: mmkarim@name.ac.bd.com